Structure and reactivity of transition metal substituted dichloroantimony and dichlorobismuth complexes †

Thomas Gröer and Manfred Scheer *

*Institut für Anorganische Chemie der Universität Karlsruhe, D-76128 Karlsruhe, Germany.
E-mail: mascheer@achibm6.chemie.uni-karlsruhe.de*

The dichloro Group 15 complexes [{Cp^x(CO)$_2$Fe}BiCl$_2$] (Cp^x = Cp, η^5-C$_5$H$_3$$tBu_2$ {Cp″}) **1a**, **b** and [{Cp″(CO)$_2$Fe}SbCl$_2$] **3** are prepared. The crystal structure determination of **1b** and **3** shows a polymeric chlorine bridged structure for the bismuth complex **1b** whereas for the antimony compound **3** a molecular structure with weak intermolecular chlorine bridges is found. The reaction of **1a** or **3** with magnesium leads to the threefold transition-metal substituted complexes [(μ$_3$-E){Fe(CO)$_2$Cp^x}$_3$] (**5**: E = Bi, Cp^x = Cp; **7**: E = Sb, Cp^x = Cp″), whereas the analogous reaction of **1b** results in the disubstituted bismuth chloro complex [{Cp″(CO)$_2$Fe}$_2$BiCl] **6**. Finally, the reaction of an equimolar mixture of **1a** and **3** with magnesium yields the novel antimony-bridged compound [(μ$_3$-Sb){Fe$_2$(μ-CO)(CO)$_2$Cp$_2$}{Fe(CO)$_2$Cp″}] **8**.

Introduction

Halogenated compounds of the heavier Group 15 elements and especially their organotransition-metal substituted derivatives have received much attention during the last two decades.[1–4] They are characterised by their unusual and often hypervalent coordination modes, which are found for example in BiCl$_3$[5] or [{Cp(CO)$_2$Fe}$_2$BiCl]$_3$.[2,6] Other examples contain ionic halogen-bridged species, *e.g.* [BiCl$_4$]$^-$,[7] [{Bi$_2$Cl$_9$}$_n$]$^{3-}$,[8] and [Bi$_2$Cl$_6${Mo(CO)$_3$Cp}$_2$]$^{2-}$.[9] Furthermore, in their reactivity pattern they mainly show the formation of main group element–transition metal clusters. A large variety of the latter complexes was achieved by the reaction of Group 15 trihalides with metalates of different complexes as well as with metal dimer compounds. This field of research is well established, as is the chemistry of dimetal-substituted halogeno bismuthanes and stibanes.[10] In contrast, only few examples of metal-substituted dihalogeno Group 15 compounds are known, yet only one of those, [{[P(OR)$_3$]$_2$(CO)$_2$Co}SbCl$_2$] (R = Me, Ph), was structurally characterised,[11] although this type of complexes was first mentioned by Cullen and co-workers as early as 1971 with the dichlorobismuth complex [{Cp(CO)$_2$Fe}BiCl$_2$].[12] Since then, studies on the reactivity of those compounds were restricted to their phosphorus analogues.[13–16]

For complexes of the type [{L$_n$M}BiCl$_2$] the occurrence is still restricted to the first example mentioned above, and one further compound synthesised by Norman and co-workers, who presented spectroscopic and analytical data for the molybdenum complex [{Cp(CO)$_3$Mo}BiCl$_2$] within their research on dimetalated monochloro bismuthanes.[3c]

We herein report on the synthesis, structures and reactivity of organotransition metal–dichlorobismuthanes [{Cp^x(CO)$_2$Fe}BiCl$_2$] (Cp^x = Cp, η^5-C$_5$H$_3$$tBu_2$ {Cp″}) **1a**, **b**, and of the dichlorostibane [{Cp″(CO)$_2$Fe}SbCl$_2$] **3**.

Results and discussion

(a) Synthesis and structure of the dichloro Group 15 complexes

The bismuth complexes [{Cp^x(CO)$_2$Fe}BiCl$_2$] (Cp^x = Cp, Cp″) **1a**, **b** were prepared by the reaction of the iron dimer
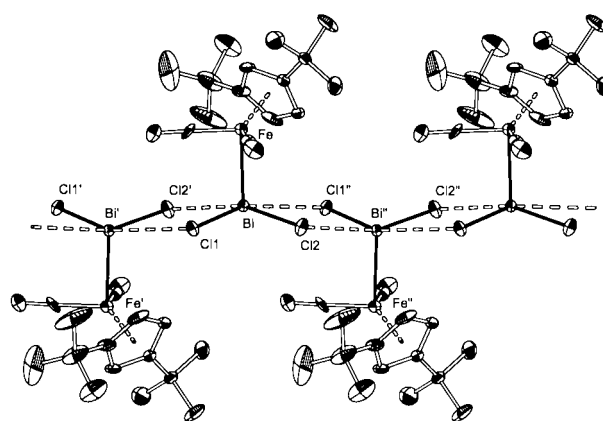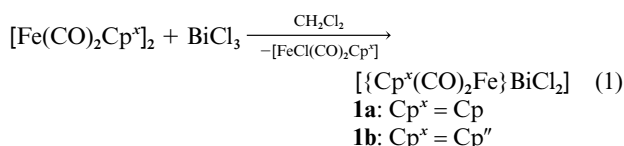
Fig. 1 Molecular structure of [{Cp″(CO)$_2$Fe}BiCl$_2$] **1b** (showing 30% probability ellipsoids; hydrogen atoms are omitted for clarity).

[{Fe(CO)$_2$Cp^x}$_2$] with BiCl$_3$ in CH$_2$Cl$_2$ as described by Cullen *et al.*[12] and isolated as orange crystals (eqn. (1)).

$$[\text{Fe(CO)}_2\text{Cp}^x]_2 + \text{BiCl}_3 \xrightarrow[-[\text{FeCl(CO)}_2\text{Cp}^x]]{\text{CH}_2\text{Cl}_2}$$

$$[\{\text{Cp}^x(\text{CO})_2\text{Fe}\}\text{BiCl}_2] \quad (1)$$

1a: Cp^x = Cp
1b: Cp^x = Cp″

Compounds **1a**, and **1b** are both insoluble in hydrocarbons and slightly soluble in polar solvents such as CH$_2$Cl$_2$, or thf. They are air-stable in the solid state and not sensitive towards moisture, whereas solutions of **1** decompose within minutes in the presence of air. Spectroscopic and analytical data of **1** were consistent with the anticipated formulae. The structure of **1b** was additionally confirmed by X-ray structure analysis (Fig. 1). Selected bond lengths and angles are given in Table 1. The structure of **1b** is polymeric, consisting of infinite one-dimensional strands of monomeric units, connected by short intermolecular bismuth–chlorine interactions [Bi···Cl 2.971(3), and 3.245(3) Å]. The strands reside on crystallographic 2$_1$-axes and can be converted into each other by 4̄-axes. This gives another example of the known Lewis acidity of three-coordinate bismuth(III), with the intermolecular Bi···Cl distances being similar to those in [PhBiCl$_2$(thf)]$_n$,[1] or [{Cp^{Me}-

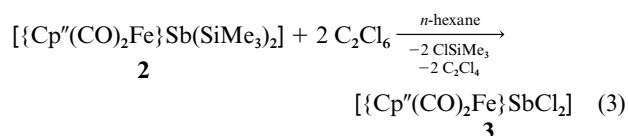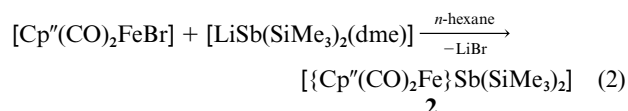DOI: 10.1039/a909394j

J. Chem. Soc., Dalton Trans., 2000, 647–653 **647**

Table 1 Selected bond lengths (Å) and angles (°) for complex **1b**

Bi–Fe	2.5847(11)	Bi · · · Cl(2′)	2.971(3)
Bi–Cl(1)	2.605(2)	Bi · · · Cl(1″)	3.245(3)
Bi–Cl(2)	2.678(2)		
Fe–Bi–Cl(1)	97.09(6)	Cl(1)–Bi–Cl(2′)	80.37(7)
Fe–Bi–Cl(2)	98.44(6)	Cl(2)–Bi–Cl(1″)	74.32(7)
Fe–Bi–Cl(2′)	97.25(6)	Cl(2′)–Bi–Cl(1″)	114.70(4)
Fe–Bi–Cl(1″)	98.70(6)	Cl(1)–Bi–Cl(1″)	156.47(4)
Cl(1)–Bi–Cl(2)	86.10(7)	Cl(2)–Bi–Cl(2′)	160.41(4)

Table 2 Selected bond lengths (Å) and angles (°) for complex **3**

Sb–Cl(1)	2.451(4)	Sb–Fe	2.508(2)
Sb–Cl(2)	2.399(4)	Sb · · · Cl(1′)	3.279(4)
Cl(1)–Sb–Fe	101.98(10)	Cl(1)–Sb–Cl(1′)	165.1(2)
Cl(2)–Sb–Fe	102.76(12)	Cl(2)–Sb–Cl(1′)	83.92(15)
Cl(1)–Sb–Cl(2)	91.30(15)		

$(CO)_3Mo\}_2BiCl]_2$[17] ($Cp^{Me} = \eta^5\text{-}C_5H_4Me$) (for other examples see refs. 1(*b*) and 18). Each Bi atom in **1b** is further connected to two chlorine atoms by short Bi–Cl bonds, whose distances [2.605(2) and 2.678(2) Å] are consistent with single bonds. In addition each Bi atom is coordinated by one Fe atom leading to the overall square-pyramidal geometry, with the Bi-atoms residing out of the plane of the chlorine atoms [angles Fe–Bi–Cl: 97.09(6)–98.70(6)°]. The iron atoms alternate on different sides of the $(BiCl_2)_\infty$ strand. Thus, the structure can be described as a chain of edge-sharing square-planar pyramids with the fifth vertex alternately pointing up or down from the chain. The only similar connectivity of chlorine bridged Bi-centres is found in the structure of the molecular compound $[Bi_2Cl_6\{Mo(CO)_3Cp\}_2]^{2-}$,[9] which represents two edge sharing $BiCl_4Mo$ square-pyramids, with the vertices pointing to two different sides of the plane of the chlorine atoms. The Bi atoms are also slightly out of the plane of Cl atoms [angles Mo–Bi–Cl: 93.4–100.7°].
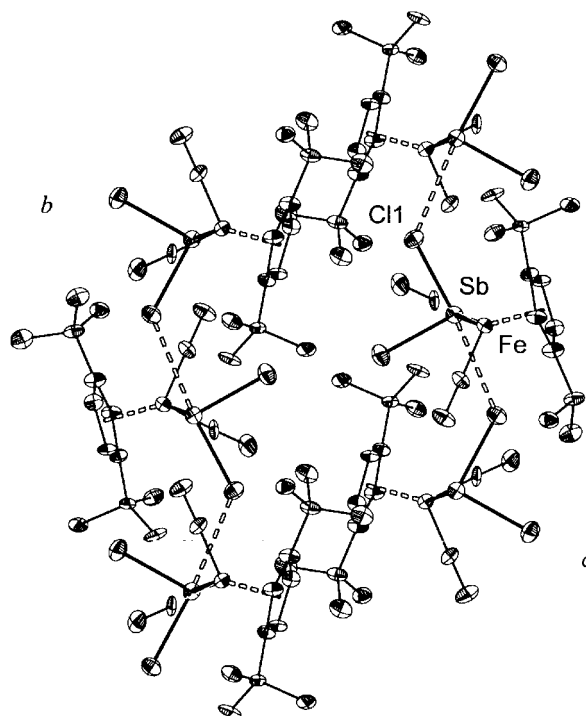
Since the formation of the antimony analogue $[\{Cp''(CO)_2Fe\}\text{-}SbCl_2]$ **3** was not feasible by the method shown in eqn. (1), we followed an analogous approach to that described by Weber *et al.* for the phosphorus compound $[\{Cp^*(CO)_2Fe\}PCl_2]$.[16] The synthesis of **3** was realised in high yields by the chlorination of the silylated antimony compound $[\{Cp''(CO)_2Fe\}Sb(SiMe_3)_2]$ **2** with C_2Cl_6. Compound **2** was prepared by the reaction of $[Cp''(CO)_2FeBr]$ with $[LiSb(SiMe_3)_2(dme)]$ (eqns. (2) and (3)).

$$[Cp''(CO)_2FeBr] + [LiSb(SiMe_3)_2(dme)] \xrightarrow[-LiBr]{n\text{-hexane}}$$
$$[\{Cp''(CO)_2Fe\}Sb(SiMe_3)_2] \quad (2)$$
$$\mathbf{2}$$

$$[\{Cp''(CO)_2Fe\}Sb(SiMe_3)_2] + 2\,C_2Cl_6 \xrightarrow[-2\,C_2Cl_4]{n\text{-hexane}}$$
$$\mathbf{2} \qquad \qquad \qquad \xrightarrow{-2\,ClSiMe_3}$$
$$[\{Cp''(CO)_2Fe\}SbCl_2] \quad (3)$$
$$\mathbf{3}$$

Compound **3** exhibits a moderate solubility in CH_2Cl_2 and is slightly soluble in hydrocarbons. The difference in its solubility compared to **1b** is caused by the different molecular structures of **1b** and **3**. Fig. 2 shows the molecular structure of **3**: selected bond lengths and angles are given in Table 2. The X-ray analysis of **3** reveals the antimony atom to be trigonal pyramidally coordinated by two chlorine atoms and one iron centre. The Sb–Cl distances [2.399(4), 2.451(4) Å] are close to the ones in the analogous compounds $[\{P(OR)_3\}_2(CO)_2Co\}SbCl_2]$ (R = Me, Ph) [2.369–2.425 Å],[11] and are within the range of known Sb–Cl distances [2.323–2.793 Å].[19,20] Hence, the molecular structure of **3** is similar to that of the monomeric unit of the Bi complex **1b**, there is, however, only one intermolecular Sb · · · Cl interaction [Sb · · · Cl(1′) 3.279(4) Å] in compound **3** (Fig. 3). This distance is 37% longer than the intramolecular Sb–Cl bond lengths, thus revealing the more molecular character of compound **3** in contrast to the strong polymeric character of **1b** (intermolecular Bi · · · Cl distances in **1b** are only 17% longer than the Bi–Cl bonds). The molecules of **3** are connected in infinite chains along the crystallographic *b*-axis, which align in sheets perpendicular to the crystallographic *c*-axis. The inter-
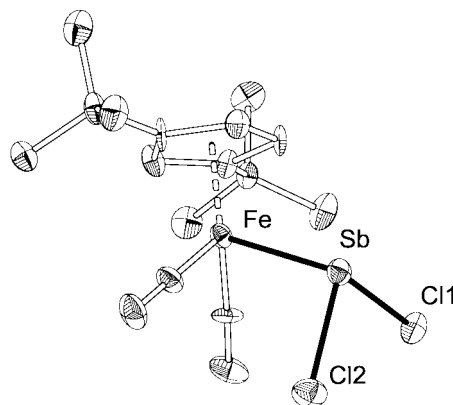
Fig. 2 Molecular structure of $[\{Cp''(CO)_2Fe\}SbCl_2]$ **3** (showing 30% probability ellipsoids; hydrogen atoms are omitted for clarity).

Fig. 3 Chains of $[\{Cp''(CO)_2Fe\}SbCl_2]$ molecules connected by intermolecular Sb · · · Cl interactions in the elementary cell of **3** (viewed along the *a*-axis, hydrogen atoms are omitted for clarity).
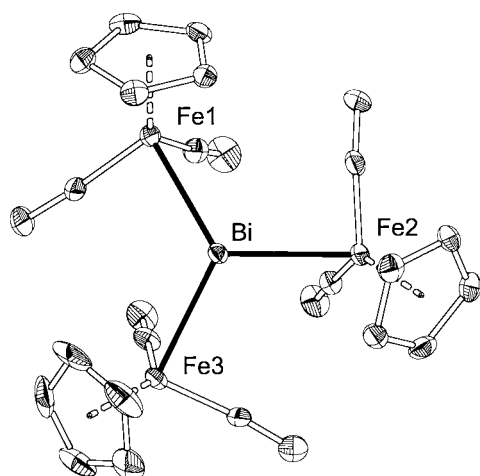
molecular Sb · · · Cl interaction causes an elongation of the Sb–Cl bond lying opposite to it of about 0.05 Å, compared to the second Sb–Cl bond. In contrast to our observations for compound **3**, Norman *et al.*[11] do not report on the occurrence of any long-range intermolecular Sb · · · Cl interactions in the analogous compounds $[\{P(OR)_3\}_2(CO)_2Co\}SbCl_2]$ (R = Me, Ph).

(b) Reactions of metal-substituted dichlorobismuthanes

Our main attention on the reactivity pattern of the dichloro complexes **1a**, **b** and **3** was focused on their reduction to

Table 3 Selected bond lengths (Å) and angles (°) for complex **5**

Bi–Fe(1)	2.7282(12)	Bi–Fe(3)	2.7172(12)
Bi–Fe(2)	2.7155(14)		
Fe(1)–Bi–Fe(2)	109.10(3)	Fe(2)–Bi–Fe(3)	107.51(4)
Fe(1)–Bi–Fe(3)	110.05(3)		

Table 4 Selected bond lengths (Å) and angles (°) for complex **6**

Bi–Fe(1)	2.6507(12)	Bi–Cl	2.604(2)
Bi–Fe(2)	2.6799(11)		
Fe(1)–Bi–Fe(2)	113.76(3)	Fe(2)–Bi–Cl	99.59(5)
Fe(1)–Bi–Cl	96.79(5)		

Fig. 4 Molecular structure of $[(\mu_3\text{-Bi})\{Fe(CO)_2Cp\}_3]$ **5** (showing 30% probability ellipsoids; hydrogen atoms are omitted for clarity).

build up E_n-cages, surrounded by metal moieties. Therefore we carried out the reduction with activated magnesium.[21]

The reaction of **1a** with an excess of magnesium in acetonitrile yields the compounds $[BiCl\{Fe(CO)_2Cp\}_2]_3$ **4** and $[(\mu_3\text{-Bi})\{Fe(CO)_2Cp\}_3]$ **5** (eqn. (4)), the former containing a planar six-membered Bi_3Cl_3 ring.
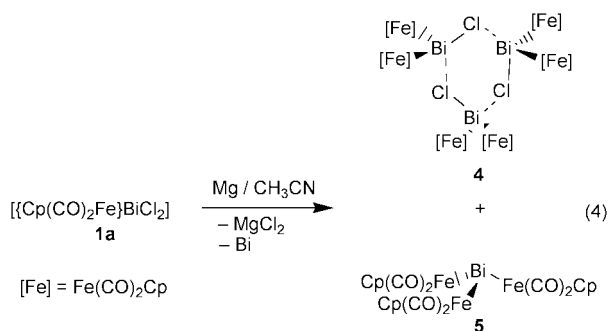

Both complexes were obtained earlier by Schmidbaur and co-workers by the reaction of $BiCl_3$ with $[Cp(CO)_2Fe]^-$.[18] Their spectroscopic data coincide with our values for both products. Even though the molecular structure of **4** was also described by Schmidbaur *et al.*, no X-ray analysis was given for complex **5**.

We were able to confirm the structure of $[(\mu_3\text{-Bi})\{Fe(CO)_2Cp\}_3]$ **5** by X-ray analysis. Selected bond lengths and angles are presented in Table 3 and the overall molecular structure is shown in Fig. 4. In **5** the bismuth atom is coordinated by three iron atoms to form a trigonal pyramid. The Bi–Fe distances are between 2.7155(14) Å and 2.7282(12) Å and therefore are within the range typical for single bonds. The Fe–Bi–Fe angles are between 107.51(4) and 110.05(3)°. In the similar compound $[(\mu_3\text{-Bi})\{Fe(CO)_2Cp^{Me}\}_3]$, for example, the averaged Fe–Bi bond distance is 2.738 Å, the mean Fe–Bi–Fe angle is 109.2°.[3] These angles are large when compared to trisubstituted organobismuthanes, *e.g.* in $BiPh_3$ the angles at bismuth are between 92 and 96°, respectively.[22] However, in organobismuth compounds with bulkier substituents, as in $Bi(Mes)_3$ (Mes = $2,4,6\text{-Me}_3C_6H_2$), larger angles were found (102.6°).[22] Hence, the observed
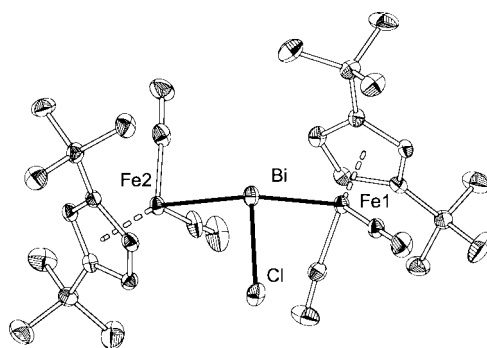
increase of the angles in **5** and $[(\mu_3\text{-Bi})\{Fe(CO)_2Cp^{Me}\}_3]$ is caused by steric effects.

Complex **1b** reacts with an excess of magnesium in THF to form $[\{Cp''(CO)_2Fe\}_2BiCl]$ **6** (eqn. (5)), no trisubstituted bismuthane was afforded.
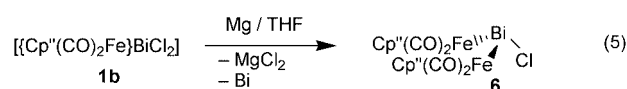

Fig. 5 shows the molecular structure of **6**: selected bond lengths and angles are given in Table 4. The structure of **6** reveals the first monomeric organoiron substituted monochlorobismuth complex bearing no intermolecular Bi · · · Cl interactions due to the steric demand of the two tertiary-butyl groups at the cyclopentadiene ligand of the iron fragments. The only other known example of a structurally characterised monomeric chlorobismuth complex is the molybdenum substituted compound $[\{Cp(CN tBu)(CO)_2Mo\}_2BiCl]$ reported by Norman *et al.*[3c] In complex **6** the bismuth atom is bonded to a terminal chlorine [Bi–Cl 2.604(2) Å] and two iron atoms (av. Bi–Fe 2.665 Å) *via* single bonds. The coordination geometry around the bismuth atom is trigonal pyramidal (sum of angles: 310.2°), in accordance with a stereochemically active lone pair.

(c) Reactions of metal-substituted dichlorostibanes

In contrast to the reaction behaviour of the bismuth complex **1b** with magnesium, the reaction of the analogous antimony complex **3** always yields the trisubstituted stibane $[(\mu_3\text{-Sb})\{Fe(CO)_2Cp''\}_3]$ **7** as a green crystalline compound (eqn. (6)).
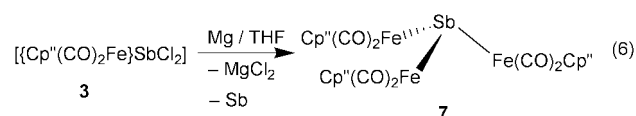
At 291 K a ^1H NMR spectrum of **7** (Table 5) reveals two singlets (δ 1.08, 1.15) in a ratio of 1:1, assigned to the methyl protons of the *tert*-butyl groups, indicating the chemically non-equivalent surrounding of these protons. In addition, the non-equivalent ring protons give rise to three broad signals (δ 4.29, 4.67 and 4.76). At a temperature of 363 K the two signals of the methyl protons as well as those of the two adjacent ring protons coalesce. Owing to the free rotation of the Cp''-ligands they are

Fig. 5 Molecular structure of $[\{Cp''(CO)_2Fe\}_2BiCl]$ **6** (showing 30% probability ellipsoids; hydrogen atoms are omitted for clarity).

Table 5 ^{1}H NMR data of **7** at different temperatures ([D$_8$]-toluene; v = 300.136 MHz)

T/K	δ(H$_{methyl}$)		δ(H$_A$)	δ(H$_{X,X'}$)	
291	1.08 (s)	1.15 (s)	4.29	4.67	4.76
343	1.11 (s)	1.15 (s)	4.31	4.70	4.75
363		1.14 (s)	4.31	4.71	

Table 6 Selected bond lengths (Å) and angles (°) for complex **7**

Sb–Fe(1)	2.6851(9)	Sb–Fe(3)	2.6838(10)
Sb–Fe(2)	2.6622(11)		
Fe(1)–Sb–Fe(2)	110.18(3)	Fe(2)–Sb–Fe(3)	111.76(3)
Fe(1)–Sb–Fe(3)	111.92(3)		
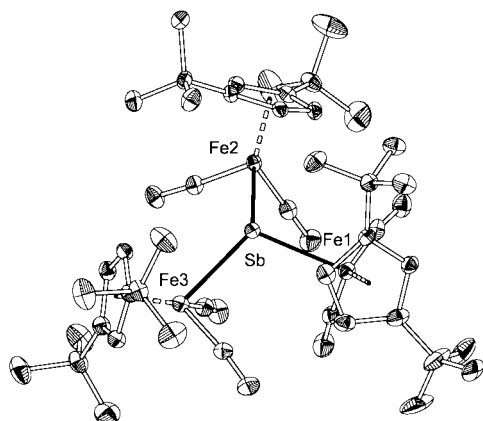
Fig. 6 Molecular structure of [(μ_3-Sb){Fe(CO)$_2$Cp''}$_3$] **7** (showing 30% probability ellipsoids; hydrogen atoms are omitted for clarity).

Table 7 Selected bond lengths (Å) and angles (°) for complex **8**

Sb–Fe(1)	2.6597(10)	Fe(2)–Fe(3)	2.6364(14)
Sb–Fe(2)	2.5793(10)	Fe(2)–C(5)	1.927(5)
Sb–Fe(3)	2.5726(10)	Fe(3)–C(5)	1.902(6)
Fe(2)–Sb–Fe(3)	61.56(4)	Sb–Fe(3)–Fe(2)	59.34(3)
Fe(1)–Sb–Fe(2)	117.51(3)	C(5)–Fe(2)–Fe(3)	46.88(16)
Fe(1)–Sb–Fe(3)	123.13(3)	C(5)–Fe(3)–Fe(2)	46.09(17)
Sb–Fe(2)–Fe(3)	59.10(3)		

Fig. 7 Molecular structure of [(μ_3-Sb){Fe$_2$(μ-CO)(CO)$_2$Cp$_2$}{Fe-(CO)$_2$Cp''}] **8** (showing 30% probability ellipsoids; hydrogen atoms are omitted for clarity).

now chemically equivalent. The free activation enthalpy of this process at coalescence temperature (T_c = 363 K) calculates to $\Delta G_{Tc}^{\#}$ = 76 kJ mol^{-1}. The structure of **7** was confirmed by X-ray analysis. Selected bond lengths and angles are given in Table 6. Fig. 6 shows the molecular structure of **7** which reveals a single antimony atom coordinated by three iron moieties in a pyramidal fashion as found for the bismuth compound **5**. The analogous compound [(μ_3-Sb){Fe(CO)$_2$Cp^{Me}}$_3$] was prepared in our group by the metalation reaction of SbCl$_3$ with three equivalents of K[Fe(CO)$_2$Cp^{Me}].[23]

The growing steric demand of the substituents at the Cp-ligand in the series of complexes [(μ_3-Sb){Fe(CO)$_2$Cp^x}$_3$] is evident in the elongation of the Sb–Fe bonds and also in the increase in the values of the Sb–Fe–Sb angles from 2.64 Å and 110.3° in [(μ_3-Sb){Fe(CO)$_2$Cp}$_3$][2] to 2.65 Å and 110.6° in [(μ_3-Sb){Fe(CO)$_2$Cp^{Me}}$_3$] to 2.68 Å and 111.3° in **7**, the latter bearing two tertiary-butyl moieties at the Cp ring.

To prove whether it is possible to form bismuth–antimony bonds in the coordination sphere of transition metals by reduction of the halogenated precursors, we studied the reaction of an equimolar mixture of [{Cp''(CO)$_2$Fe}BiCl$_2$] **1a** and [{Cp''-(CO)$_2$Fe}SbCl$_2$] **3** with magnesium. We chose different Cp ligands on the different main-group elements to ensure an unambiguous identification of the corresponding element in the products by means of NMR spectroscopy and X-ray diffraction, respectively, as well as to get an insight into a possible Cp migration process. During reaction (7) a black precipitate
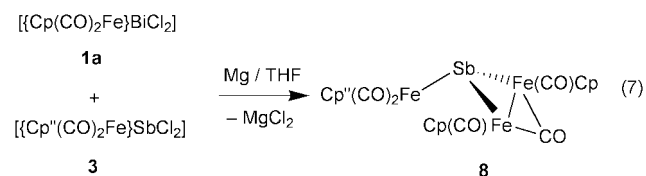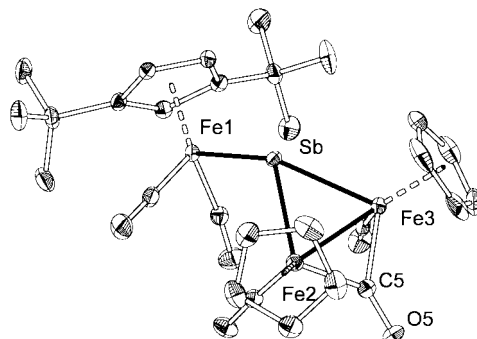
[{Cp(CO)$_2$Fe}BiCl$_2$]

1a

+

[{Cp''(CO)$_2$Fe}SbCl$_2$]

3

$$\xrightarrow[\text{– MgCl}_2]{\text{Mg / THF}}$$ (7)

8

was formed. After work-up of the solution, dark red crystals were obtained for which spectroscopic, X-ray and analytical data were consistent with the formula [(μ_3-Sb){Fe$_2$(μ-CO)-(CO)$_2$Cp$_2$}{Fe(CO)$_2$Cp''}] **8**. The IR-spectrum of **8** (KBr) reveals five bands in the region of terminal CO-groups. In addition two further bands (1794 and 1784 cm^{-1}) for the bridging carbonyl ligand are observed.

The product of reaction (7) contains not only the Fe(CO)$_2$-Cp''-fragment originating from the antimony containing starting material **3** but also two FeCp-moieties from **1a**, which excludes the formation of **8** via an intermediate generation of [(μ_3-Sb){Fe(CO)$_2$Cp''}$_3$] followed by a subsequent loss of a CO group. The reaction rather proceeds by a cleavage of the Fe–Bi-bond with the generation of [Cp(CO)$_2$Fe]$^-$ nucleophiles. Hence, a possible reaction pathway is the metalation of **3** with precipitation of elemental bismuth.

A ^{1}H NMR spectrum of **8** reveals three signals due to the protons of the substituted Cp'' ligand [δ 1.21 (s), 4.76 (d), 4.87 (t)]. A further singlet at δ 4.38 indicates the presence of two equivalent Cp moieties. Fig. 7 shows the molecular structure of **8**: selected bond lengths and angles are given in Table 7. The structure of **8** reveals antimony in a distorted trigonal pyramidal coordination mode of three iron atoms [Fe(2)–Sb–Fe(3) 61.56(4)°, Fe(1)–Sb–Fe(2) 117.51(3), Fe(1)–Sb–Fe(3) 123.13(3)°]. In contrast to the situation in [(μ_3-Sb){Fe(CO)$_2$Cp''}$_3$] **7**, the antimony atom is in a bridging function at the Fe$_2$(CO)$_3$Cp$_2$ fragment. Alternatively, compound **8** can be described as to be derived from the dimeric complex [Fe(CO)$_2$Cp]$_2$ by replacement of a bridging carbonyl group by a SbFe(CO)$_2$Cp'' moiety. A few examples for bridging antimony species are found in complexes like [{(μ_4-Sb)Fe$_2$(CO)$_8$}$_2${Fe$_2$(CO)$_6$}],[24] [(μ_4-Sb){Fe$_2$(CO)$_6$(μ-CO)$_2$}-{Fe(CO)$_4$}{Cr(CO)$_5$}],[25] or [NEt$_4$][(μ_4-Sb){Fe$_2$(CO)$_8$}-{Fe(CO)$_4$}$_2$][26] where antimony is tetra-coordinated in a disphenoidal manner, whereas in none of these examples threefold coordinated antimony can be found. The Sb–Fe bond distances of the Fe$_2$Sb triangle in **8** are almost equal [Sb–Fe(2) 2.5793(10) and Sb–Fe(3) 2.5726(10) Å] and significantly shorter than the bond distance to the terminal iron atom [Sb–Fe(1) 2.6597(10) Å].
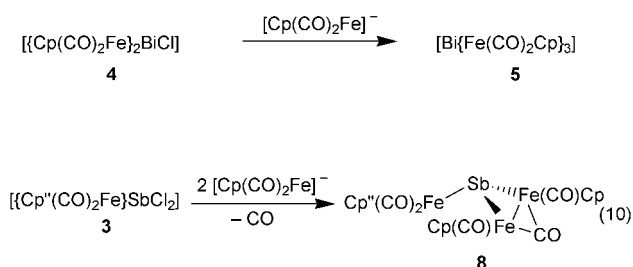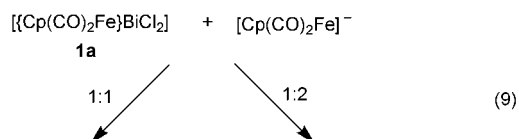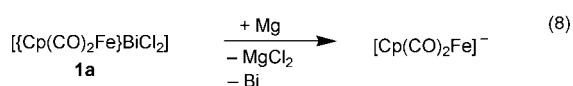
The arrangement of the Cp ligands at the iron atoms in **8** is similar to that in cis-[Fe(CO)$_2$Cp]$_2$. The Fe–Fe distance [Fe(2)–Fe(3) 2.6364(14) Å] is elongated by 0.1 Å compared to that in

cis-[Fe(CO)$_2$Cp]$_2$ [2.531 Å].[27b] The Fe–Fe bond in **8** is additionally bridged symmetrically by one CO group [Fe(2)–C(5) 1.927(5), and Fe(3)–C(5) 1.902(6) Å] and there is no significant difference from usual Fe–C distances of μ-bridging CO groups.[27–31]

In **8** the two planes Fe(2)–Fe(3)–C(5) and Fe(2)–Fe(3)–Sb are bent by 159.9°, which is also found for compounds of the type *cis*-[Fe(μ-CO)(CO)Cp^x]$_2$ (Cp^x = Cp: 164°,[27b] Cp″: 157°[30]). Analogous compounds with *trans* arrangement of the Cp^x-ligands (Cp^x = Cp,[27a] η^5-C$_5$H$_4$$t$Bu,[30] Cp*[31]) possess a planar Fe$_2$C$_2$ core.

(d) Discussion of the reaction pathway

In the reactions of the dichloroantimony and the dichlorobismuth compounds **1a**, **b** and **3** with magnesium no element–element bonds are formed, whereas we find an iron–element bond formation with the precipitation of elemental antimony and bismuth, respectively. These observations lead to the reaction pathway shown in eqns. (8)–(10).

$$[\{Cp(CO)_2Fe\}BiCl_2] \xrightarrow[\substack{- MgCl_2 \\ - Bi}]{+ Mg} [Cp(CO)_2Fe]^- \qquad (8)$$
$$\mathbf{1a}$$

$$[\{Cp(CO)_2Fe\}BiCl_2] + [Cp(CO)_2Fe]^-$$
$$\mathbf{1a}$$

$$1{:}1 \swarrow \qquad \searrow 1{:}2 \qquad (9)$$

$$[\{Cp(CO)_2Fe\}_2BiCl] \xrightarrow{[Cp(CO)_2Fe]^-} [Bi\{Fe(CO)_2Cp\}_3]$$
$$\mathbf{4} \qquad\qquad\qquad \mathbf{5}$$

$$[\{Cp''(CO)_2Fe\}SbCl_2] \xrightarrow[- CO]{2\,[Cp(CO)_2Fe]^-} Cp''(CO)_2Fe\overset{Sb}{\underset{Cp(CO)Fe}{\diamond}}\overset{Fe(CO)Cp}{\underset{CO}{}} \quad (10)$$
$$\mathbf{3} \qquad\qquad\qquad\qquad\qquad\qquad \mathbf{8}$$

Obviously Mg cleaves the element–iron bonds in the starting materials to generate anionic [Fe(CO)$_2$Cp^x]$^-$ (Cp^x = Cp, Cp″) (eqn. (8)), which will attack further starting material as a nucleophile and subsequently form the iron rich complexes **4**–**7** (eqn. (9)). It is interesting to note, that in the reduction reaction (7) of a mixture of the bismuth and antimony starting complexes **1a** and **3** only the antimony containing species **8** was formed in high yields, containing iron fragments from the bismuth and the antimony starting material, whereas no bismuth containing species was found. This indicates the stronger metallic character of bismuth, as well as the preferred Bi–Fe bond cleavage followed by subsequent metalation of the dichloroantimony compound **3** by the thus generated [Fe(CO)$_2$Cp]$^-$ fragments (eqn. (10)).

Conclusions

The results show that independent from the substitution pattern at the Cp^x-ligand, transition-metal substituted dichlorobismuthanes of the type [{Cp^x(CO)$_2$Fe}BiCl$_2$] will adopt polymeric structures revealing the tendency of bismuth to adopt a hypervalent coordination sphere. In contrast therefore, the antimony analogue [{Cp″(CO)$_2$Fe}SbCl$_2$] reveals a more monomeric character with a lower tendency to adopt hypervalent coordination.

Attempts to reduce these chlorinated bismuthanes and stibanes to form element–element bonds results in metal–element bond cleavage and the generation of a higher transition-metal substitution at the Group 15 element with a concomitant precipitation of the element. These tendencies are different to the behaviour of analogous arsenic and phosphorus compounds, which is caused by the stronger metallic character of antimony and bismuth in comparison to arsenic and phosphorus.

Therefore other synthetic routes, like dehalogenosilylation or dehydrosilylation reactions, should be employed to build up larger main group element clusters.

Experimental

General procedures

All manipulations were performed under an atmosphere of dry Ar using standard Schlenk techniques. All solvents were dried by common methods and freshly distilled prior to use. Bismuth trichloride was obtained commercially and used without further purification. Activated magnesium was donated by Professor B. Bogdanović.[21] The compounds [Fe(CO)$_2$Cp^x]$_2$ (Cp^x = Cp, Cp″, Cp*),[30] [Cp″(CO)$_2$FeBr][32] and [LiSb(SiMe$_3$)$_2$(dme)$_n$][33] were prepared according to literature methods, the dme content of the latter compound was determined by ^{1}H NMR spectroscopy. NMR spectra were recorded on a Bruker AC 250 (^{1}H, ^{13}C, ^{29}Si), and a Bruker AMX 300 (^{1}H) using SiMe$_4$ as external standard, the IR spectra were recorded on a Bruker IFS 28. Mass spectroscopy was carried out on a Varian MAT 711, elemental analysis on an Elementar Vario EL.

Preparations

[{Cp^x(CO)$_2$Fe}BiCl$_2$] (Cp^x = Cp, Cp″) 1a, b. According to literature methods,[12b] BiCl$_3$ (4.16 g, 13.2 mmol or 1.61 g, 5.1 mmol) was added to a vigorously stirred solution of [Fe(CO)$_2$Cp]$_2$ (4.67 g, 13.2 mmol) or [Fe(CO)$_2$Cp″]$_2$ (2.97 g, 5.1 mmol), respectively, in 50 ml of CH$_2$Cl$_2$. After 18 h all BiCl$_3$ had dissolved and an orange precipitate had formed. The residual solution was then filtered off and the precipitate washed three times with 10 ml of Et$_2$O. The so obtained microcrystalline solid was analytically pure. Crystals of **1b** suitable for X-ray diffraction were obtained by reducing the mother-liquor and storing it at 0 °C (5.005 g, 83% for **1a** and 3.825, 75% for **1b**). **1a** (Found: C, 18.80; H, 1.28; C$_7$H$_5$Bi-Cl$_2$FeO$_2$ requires C, 18.40; H, 1.10%); MS (70 eV, EI) *m/z* (%): 456.0 (3.2) [M$^+$], 428.0 (4.8) [M$^+$ − CO], 421 (4.1) [M$^+$ − Cl], 400 (10.8) [M$^+$ − 2(CO)], 279 (96.5) [BiCl$_2^+$], 121 (31.2) [FeCp$^+$]; ^{1}H NMR ([D$_8$]-THF): δ 5.12 (s); IR (KBr, cm^{-1}): 2081 (m), 2071 (s), 2059 (vs), 2039 (w), 2013 (vs), 1986 (m). **1b** (Found: C, 32.21; H, 3.77; C$_{15}$H$_{21}$BiCl$_2$FeO$_2$ requires C, 31.66; H, 3.72%); MS (70 eV EI) *m/z* (%): 568 (0.84) [M$^+$], 533 (1.51) [M$^+$ − Cl], 410 (13.78) [FeCp″$_2^+$], 268 (49.9) [FeClCp″$^+$], 386 (6.01) [BiCp″$^+$]; ^{1}H NMR ([D$_8$]-THF): δ 1.27 (s, 18H), 4.81 (t, 1H, *J* = 1.7 Hz), 5.09 (d, 2H, *J* = 1.7 Hz); IR (KBr, cm^{-1}) ṽ (CO): 2032 (w), 2007 (s), 2000 (s), 1990 (w), 1980 (w), 1958 (vs).

[{Cp″(CO)$_2$Fe}SbCl$_2$] 3. To a slurry of [Cp″(CO)$_2$FeBr] (2.506 g, 6.8 mmol) in *n*-hexane at 0 °C [LiSb(SiMe$_3$)$_2$(dme)] (2.481 g, 5.4 mmol) was added in small portions over 1 h. This resulted in a red solution which was allowed to warm to room temperature and was stirred for another 12 h. After filtering all volatiles were removed *in vacuo*, the resulting red solid was analytically (^{1}H NMR) pure [{Cp″(CO)$_2$Fe}Sb(SiMe$_3$)$_2$] (**2**) and was used to prepare **3** without further purification.

In a second step C$_2$Cl$_6$ (2.3 g, 9.8 mmol) was added at once to the solution of **2** (2.73 g, 4.9 mmol) in 50 ml of *n*-hexane. Within 12 h of stirring all C$_2$Cl$_6$ slowly dissolved and a dark coloured precipitate formed. This was filtered off and washed several times with 10 ml of *n*-hexane. Subsequently the solid was extracted with 30 ml CH$_2$Cl$_2$ until the extract was colourless. The resulting yellow solution was reduced to dryness producing **3** as a yellow powder. Crystals of **3** suitable for

Table 8 Crystallographic data for **1b**, **3**, **5**, **6**, **7** and **8**

	1b	3	5·CH₃CN	6	7	8
Empirical formula	$C_{15}H_{21}BiCl_2FeO_2$	$C_{15}H_{21}Cl_2FeO_2Sb$	$C_{23}H_{18}BiFe_3O_6N$	$C_{30}H_{42}BiClFe_2O_4$	$C_{45}H_{63}Fe_3O_6Sb$	$C_{28}H_{31}Fe_3O_5Sb$
M_r	569.05	481.82	780, 92	822.77	989.25	736.83
T/K	200(1)	200(1)	193(1)	200(1)	190(1)	200(1)
Space group	$I\bar{4}$	$P2_1/c$	$P2_1/n$	$P2_1/n$	$P2_1/c$	$P\bar{1}$
Crystal system	Tetragonal	Monoclinic	Monoclinic	Monoclinic	Monoclinic	Triclinic
a/Å	20.936(3)	11.919(2)	8.144(2)	10.479(2)	15.015(3)	6.9597(14)
b/Å	20.936(3)	10.089(2)	18.352(4)	15.405(3)	10.748(2)	13.363(3)
c/Å	8.9426(18)	15.006(3)	16.518(3)	20.248(4)	29.927(6)	15.702(3)
α/°						73.79(3)
β/°		94.68(3)	92.53(3)	98.84(3)	103.12(3)	89.82(3)
γ/°						88.65(3)
V/Å⁻³	3875.9(11)	1798.5(6)	2466.3(9)	3229.9(11)	4703.5(16)	1401.8(5)
Z	8	4	4	4	4	2
μ(Mo-Kα)/mm⁻¹	10.092	2.606	8.881	6.435	1.517	2.510
Reflections collected	11852	12507	10636	20177	28787	8561
Independent reflections	3727	3387	4566	5830	9125	5017
	(R_{int} = 0.0579)	(R_{int} = 0.2769)	(R_{int} = 0.0802)	(R_{int} = 0.0728)	(R_{int} = 0.0685)	(R_{int} = 0.0306)
Reflections with $I > 2\sigma(I)$	3267	1341	3903	5080	6609	4011
Final R_1, wR_2 ($I > 2\sigma(I)$)	0.0306, 0.0648	0.0716, 0.1170	0.0520, 0.1319	0.0513, 0.1371	0.0475, 0.1086	0.0334, 0.0823
(all data)	0.0383, 0.0666	0.1613, 0.2047	0.0579, 0.1362	0.0567, 0.1409	0.0765, 0.1298	0.0479, 0.1027

X-ray diffraction could be obtained by crystallisation from a saturated CH_2Cl_2 solution at 0 °C (2.73 g, 72% for **2** and 1.81 g, 67% for **3**). **2**: NMR (C_6D_6), ¹H: δ 0.53 (s, 18H, SiCH), 1.14 (s, 18H, CCH), 5.14 (m, 1H), 5.18 (m, 2H); ²⁹Si: −11.27 (dec, $^2J_{HSi}$ = 6.7 Hz); IR (*n*-hexane, cm⁻¹): $\tilde{v}$(CO) 1995 (vs), 1950 (s). **3** (Found: C, 37.22; H, 4.40; $C_{15}H_{21}Cl_2FeO_2Sb$ requires C, 37.39; H, 4.39%); MS (70 eV EI) *m/z* (%): 482.1 (0.7) [M⁺], 454.1 (0.6) [M⁺ − CO], 370.2 (9.7) [Cp″SbCl₂⁺], 335.2 (17.2) [Cp″SbCl⁺], 193.0 (39.0) [SbCl₂⁺]; NMR (CDCl₃) ¹H: δ 1.29 (s, 18H), 4.52 (d, 2H, $^4J_{HH}$ = 1.7 Hz), 4.89 (t, 1H, $^4J_{HH}$ = 1.7 Hz); ¹³C: 31.3 (CCH₃), 31.7 (CH₃), 80.85 (C₅); IR (KBr, cm⁻¹): $\tilde{v}$(CO) 2112 (w), 2037 (s), 2016 (m), 1992 (s).

[Bi{Fe(CO)₂Cp}₃] 5. To a solution of **1a** (0.46 g, 1 mmol) in acetonitrile was added an excess of activated magnesium (0.04 g, 2 mmol). After stirring for 12 h the solution had changed colour from red to dark green. After filtering off residual Mg, the filtrate was reduced to dryness and extracted with 50 ml of *n*-hexane over a column (10 × 2 cm) of dry SiO₂. The resulting solution was reduced to 15 ml and at −20 °C green crystals of **5** formed (0.155 g, 21%, theoretical yield is 33%, based on **1a**). IR, ¹H NMR, and analytical data are consistent with literature values.[6] Further crystallisation afforded a little [{Cp(CO)₂Fe}₂-BiCl]₃ (**4**) (30 mg, 18%). **5** (Found: C, 33.92; H, 2.20; $C_{21}H_{15}$-$BiFe_3O_6$ requires C, 34.09; H, 2.04%); ¹H NMR (CDCl₃): δ 5.01 (s, 15H); IR (CH_2Cl_2, cm⁻¹): $\tilde{v}$(CO) 1999 (s), 1995 (sh), 1970 (s), 1929 (s).

[{Cp″(CO)₂Fe}₂BiCl] 6. The synthetic procedure is analogous to the preparation of **5**. Materials are: **1b** (0.327 g, 0.6 mmol), activated magnesium (0.03 g, 1.3 mmol), THF 50 ml, which gives 0.212 g of **6** (43% based on **1b**). MS (70 eV EI) *m/z* (%): 822.2 (0.5) [M⁺], 533.0 (0.1) [BiClFe(CO)₂Cp″⁺], 289.1 (4.0) [Fe(CO)₂Cp″⁺], 268.1 (76.4) [FeClCp″⁺]; ¹H NMR (C_6D_6): δ 1.01 (s, 36H), 5.14 (br, 4H), 5.18 (br, 2H); IR (KBr, cm⁻¹): $\tilde{v}$(CO) 1999 (s), 1967 (m), 1931 (m), 1897 (s).

[Sb{Fe(CO)₂Cp″}₃] 7. To a solution of [{Cp″(CO)₂Fe}SbCl₂] **3** (0.36 g, 0.7 mmol) in 50 ml of THF activated magnesium (0.04 g, 1.4 mmol) is added at once under vigorous stirring. After 12 h the reaction mixture is reduced to dryness, the brown residue extracted twice with 20 ml of hexane. The resulting brown solution is reduced to 10 ml and stored at 0 °C. After a few days dark green crystals of [Sb{Fe(CO)₂Cp″}₃] **7** can be isolated (0.150 g, 22%, theoretical yield is 33%, based on **3**) (Found: C, 54.45; H, 6.57; $C_{45}H_{63}Fe_3O_6Sb$ requires C, 54.63; H,

6.41%); MS (70 eV EI) *m/z* (%): 989.2 (0.1) [M⁺], 960.2 (0.5) [M⁺ − CO], 932.2 (3.1) [M⁺ − 2(CO)], 820.2 (9.3) [M⁺ − 6(CO)], 578.2 (69.2) [{Fe(CO)₂Cp″}₂⁺]; ¹H NMR ([D₈]-toluene) at 291 K: δ 1.08 (s, 27H); 1.15 (s, 27H); 4.29 (br, 3H); 4.67 (br, 3H); 4.76 (br, 3H); at 363 K: 1.14 (s, 54H), 4.31 (br, 3H), 4.71 (br, 6H); IR (KBr, cm⁻¹): $\tilde{v}$(CO) 2013 (m), 2007 (s), 1977 (m), 1966 (m), 1931 (s).

[(μ₃-Sb){Fe₂(μ-CO)(CO)₂Cp₂}{Fe(CO)₂Cp″}] 8. A solution of equimolar amounts of [{Cp″(CO)₂Fe}SbCl₂] **3** (0.39 g, 0.4 mmol) and [{Cp(CO)₂Fe}BiCl₂] **1a** (0.37 g, 0.4 mmol) in THF was treated with activated magnesium (0.09 g, 3.7 mmol). After 12 h of stirring the colour of the solution had changed to brown and a black precipitate formed. All volatile compounds were removed *in vacuo* and the residue was suspended in 20 ml of *n*-hexane. After filtering off any non-soluble compounds, red crystals of [(μ₃-Sb){Fe₂(μ-CO)(CO)₂Cp₂}{Fe(CO)₂Cp″}] **8** could be isolated from the resulting filtrate at 0 °C (0.092 g, 31%, theoretical yield is 50%, based on **3**) (Found: C, 45.44; H, 4.41; $C_{28}H_{31}Fe_3O_5Sb$ requires C, 45.64; H, 4.24%); MS (70 eV EI) *m/z* (%): 735.93 (1.8) [M⁺], 707.95 (0.8) [M⁺ − CO], 679.96 (0.6) [M⁺ − 2(CO)], 651.96 (0.4) [M⁺ − 3(CO)], 623.97 (4.3) [M⁺ − 4(CO)], 595.97 (1.5) [M⁺ − 5(CO)], 298.0 (22.3) [Fe₂(CO)₂Cp₂⁺], 289.10 (39.4) [Fe(CO)₂Cp″⁺], 261.10 (29.8) [FeCOCp″⁺], 233.10 (82.5) [FeCp″⁺], 121.0 (48.2) [FeCp⁺]; NMR (C_6D_6) ¹H: δ 1.21 (s, 18H, CH₃), 4.38 (s, 10H, C_5H_5), 4.76 (d, 2H, $^4J_{HH}$ = 1.8 Hz), 4.87 (t, 1H, $^4J_{HH}$ = 1.8 Hz); ¹³C: δ 31.92 (CCH₃), 32.57 (CH₃), 83.01 and 83.16 ($C_5H_3tBu_2$), 85.42 (C_5H_5), 215.63 and 217.65 (CO); IR (KBr, cm⁻¹): $\tilde{v}$(CO) 2011 (s), 2001 (m), 1977 (s), 1966 (sh), 1939 (m), 1931 (m), 1794 (w), 1784 (w).

X-Ray structure determinations

Data were collected on a STOE IPDS diffractometer. The structures were solved using the programs SHELXS-86[34a] and SHELXL-93.[34b] All non-hydrogen atoms were refined aniso-tropically (except those of the solvent molecule in **5**). The Flack parameter of the acentric structure of **1b** came to a value of −0.035(9). Furthermore the high rest electron density in the structure of **6** is located at a distance of 2.219(6) Å from the central Bi atom. Attempts to refine this electron density as a distorted Cl atom in a ratio of 20/80 (compared to the original Cl atom) leads to a further improvement of the final structural parameters (R_1 = 0.0439 and wR_2 (all data) = 0.1223). Crystallographic data are given in Table 8.

CCDC reference number 186/1813.

Acknowledgements

References

1 (a) N. C. Norman, *Phosphorus, Sulfur Silicon*, 1994, **87**, 167; (b) W. Clegg, N. A. Compton, R. J. Errington, G. A. Fisher, D. C. R. Hockless, N. C. Norman, N. A. L. Williams, S. E. Stratford, S. J. Nichols, P. S. Jarrett and A. G. Orpen, *J. Chem. Soc., Dalton Trans.*, 1992, 193.

2 A. M. Barr, M. D. Kerlogue, N. C. Norman, P. M. Webster and L. J. Farrugia, *Polyhedron*, 1989, **8**, 2495.

3 W. Clegg, N. A. Compton, R. J. Errington and N. C. Norman, (a) *J. Chem. Soc., Dalton Trans.*, 1988, 1671; (b) *Polyhedron*, 1987, **6**, 2031; (c) W. Clegg, N. A. Compton, R. J. Errington, N. C. Norman and A. J. Tucker, *J. Chem. Soc., Dalton Trans.*, 1988, 2941.

4 C. J. Carmalt, L. J. Farrugia and N. C. Norman, *J. Chem. Soc., Dalton Trans.*, 1996, 455.

5 S. C. Nyburg, G. A. Ozin and J. T. Szymanksi, *Acta Crystallogr., Sect. B*, 1971, **27**, 2298.

6 J. M. Wallis, G. Müller and H. Schmidbaur, *J. Organomet. Chem.*, 1987, **325**, 159.

7 N. J. Mammano, A. Zalkin, A. Landers and A. L. Rheingold, *Inorg. Chem.*, 1977, **16**, 297.

8 K. Kihara and T. Sudo, *Acta Crystallogr., Sect. B*, 1974, **30**, 1088.

9 R. J. Errington, G. A. Fisher, N. C. Norman, A. G. Orpen and S. E. Stratford, *Z. Anorg. Allg. Chem.*, 1994, **620**, 457.

10 For reviews see M. Scheer and E. Hermann, *Z. Chem.*, 1990, **30**, 41; O. J. Scherer, *Angew. Chem., Int. Ed. Engl.*, 1990, **29**, 1104; K. H. Whitmire, *Adv. Organomet. Chem.*, 1998, **42**, 1.

11 N. C. Norman, P. M. Webster and L. J. Farrugia, *J. Organomet. Chem.*, 1992, **430**, 205.

12 (a) W. R. Cullen, D. J. Patmore, J. R. Sams, M. J. Newlands and L. K. Thompson, *Chem. Commun.*, 1971, 952; (b) W. R. Cullen, D. J. Patmore and J. R. Sams, *Inorg. Chem.*, 1973, **12**, 867.

13 (a) E. A. V. Ebsworth, N. T. McManus and D. W. H. Rankin, *J. Chem. Soc., Dalton Trans.*, 1984, 2573; (b) E. A. V. Ebsworth, R. O. Gould, N. T. McManus, N. J. Pilkington and D. W. H. Rankin, *J. Chem. Soc., Dalton Trans.*, 1984, 2561; (c) E. A. V. Ebsworth, N. T. McManus, D. W. H. Rankin and J. D. Whitelock, *Angew. Chem., Int. Ed. Engl.*, 1981, **20**, 801; (d) E. A. V. Ebsworth, R. O. Gould, N. T. McManus, N. J. Pilkington, D. W. H. Rankin, M. D. Walkinshaw and J. D. Whitelock, *J. Organomet. Chem.*, 1983, **249**, 227.

14 W. Malisch and R. Alsmann, *Angew. Chem., Int. Ed. Engl.*, 1976, **15**, 769.

15 V. Grossbruchhaus and D. Rehder, *Inorg. Chim. Acta*, 1990, **172**, 141.

16 L. Weber and U. Sonnenberg, *Chem. Ber.*, 1991, **124**, 725.

17 C. J. Carmalt, W. Clegg, M. R. J. Elsegood, R. J. Errington, J. Havelock, P. Lightfoot, N. C. Norman and A. J. Scott, *Inorg. Chem.*, 1996, **35**, 3709.

18 J. M. Wallis, G. Müller and H. Schmidbaur, *J. Organomet. Chem.*, 1987, **325**, 159.

19 B. Sigwarth, U. Weber, L. Zsolnai and G. Huttner, *Chem. Ber.*, 1985, **118**, 3114.

20 R. Hulme and J. C. Scruton, *J. Chem. Soc. A*, 1968, 2449.

21 For a description of the synthesis of activated magnesium see: B. Bogdanović, *Angew. Chem., Int. Ed. Engl.*, 1985, **24**, 262; E. Bartmann, B. Bogdanović, N. Janke, S. Liao, K. Schlichte, B. Spliethoff, J. Treber, U. Westeppe and U. Wilczock, *Chem. Ber.*, 1990, **123**, 1517; E. Bartmann, B. Bogdanović, N. Janke, S. Liao, K. Schlichte, B. Spliethoff, J. Treber, U. Westeppe and U. Wilczok, *Synthetic Methods of Organometallic and Inorganic Chemistry*, G. Thieme, Stuttgart, 1996, vol. 1, pp. 38ff.

22 D. M. Hawley and G. Ferguson, *J. Chem. Soc. A*, 1968, 2059; A. N. Sobolev, I. D. Romm, V. K. Belskii and E. N. Guryanova, *Koord. Khim.*, 1980, **6**, 945.

23 U. Vogel, G. Baum and M. Scheer, *Z. Anorg. Allg. Chem.*, 2000, **626**, in the press.

24 A. M. Arif, A. H. Cowley and M. Pakulski, *J. Chem. Soc., Chem. Commun.*, 1987, 622; A. L. Rheingold, S. J. Geib, M. Shieh and K. H. Whitmire, *Inorg. Chem.*, 1987, **26**, 463.

25 K. H. Whitmire, M. Shieh and J. Cassidy, *Inorg. Chem.*, 1989, **28**, 3164.

26 S. Luo and K. H. Whitmire, *J. Organomet. Chem.*, 1989, **376**, 297.

27 (a) R. F. Bryan and P. T. Greene, *J. Chem. Soc. A*, 1970, 3064; (b) R. F. Bryan, P. T. Greene, M. J. Newlands and D. S. Field, *J. Chem. Soc. A*, 1970, 3086.

28 F. A. Cotton and J. M. Troup, *J. Am. Chem. Soc.*, 1974, **96**, 4155.

29 F. A. Cotton and J. M. Troup, *J. Chem. Soc., Dalton Trans.*, 1974, 800.

30 M. Scheer, K. Schuster, U. Becker, A. Krug and H. Hartung, *J. Organomet. Chem.*, 1993, **460**, 105.

31 R. G. Teller and J. M. Williams, *Inorg. Chem.*, 1980, **19**, 2770.

32 R. B. King, W. M. Douglas and E. Efraty, *J. Organomet. Chem.*, 1974, **69**, 131.

33 G. Becker, G. Gutekunst and H.-J. Wessely, *Z. Anorg. Allg. Chem.*, 1980, **462**, 113; G. Becker, A. Münch and C. Witthauer, *Z. Anorg. Allg. Chem.*, 1982, **492**, 15.

34 (a) G. M. Sheldrick, SHELXS-86, University of Göttingen, 1986; (b) G. M. Sheldrick, SHELXL-93, University of Göttingen, 1993.

Paper a909394j